Neurochemical Research (2019) 44:2170–2181
https://doi.org/10.1007/s11064-019-02856-8

ORIGINAL PAPER

Elevated Neuroglobin Lessens Neuroinflammation and Alleviates Neurobehavioral Deficits Induced by Acute Inhalation of Combustion Smoke in the Mouse

Murat F. Gorgun[1] · Ming Zhuo[1] · Kelly T. Dineley[2,3,4] · Ella W. Englander[1,5]

Received: 23 May 2019 / Revised: 3 July 2019 / Accepted: 5 August 2019 / Published online: 16 August 2019
© Springer Science+Business Media, LLC, part of Springer Nature 2019

Abstract

Acute inhalation of combustion smoke produces long-term neurologic deficits in survivors. To study the mechanisms that contribute to the development of neurologic deficits and identify targets for prevention, we developed a mouse model of acute inhalation of combustion smoke, which supports longitudinal investigation of mechanisms that underlie the smoke induced inimical sequelae in the brain. Using a transgenic mouse engineered to overexpress neuroglobin, a neuroprotective oxygen-binding globin protein, we previously demonstrated that elevated neuroglobin preserves mitochondrial respiration and attenuates formation of oxidative DNA damage in the mouse brain after smoke exposure. In the current study, we show that elevated neuronal neuroglobin attenuates the persistent inflammatory changes induced by smoke exposure in the mouse brain and mitigates concordant smoke-induced long-term neurobehavioral deficits. Specifically, we found that increases in hippocampal density of GFAP and Iba-1 positive cells that are detected post-smoke in wild-type mice are absent in the neuroglobin overexpressing transgenic (Ngb-tg) mice. Similarly, the smoke induced hippocampal myelin depletion is not observed in the Ngb-tg mice. Importantly, elevated neuroglobin alleviates behavioral and memory deficits that develop after acute smoke inhalation in the wild-type mice. Taken together, our findings suggest that the protective effects exerted by neuroglobin in the brains of smoke exposed mice afford protection from long-term neurologic sequelae of acute inhalation of combustion smoke. Our transgenic mouse provides a tool for assessing the potential of elevated neuroglobin as possible strategy for management of smoke inhalation injury.

Keywords Neuroglobin · Neuroprotection · Neuroinflammation · Combustion smoke inhalation brain injury · Neurogenesis · Novel object recognition

Introduction

Neuroglobin is an evolutionarily ancient oxygen binding heme protein [1, 2]. In the mammalian nervous system neuroglobin localizes primarily to neuronal cytosol and its expression varies in a brain region specific manner [3–5]. Although since its discovery nearly 20 years ago [1], neuroglobin has been repeatedly implicated in neuroprotection, the mechanisms underlying its ameliorative effects in the many models of brain and neuronal injuries have not been fully elucidated [5–8]. Examples of proposed neuroprotective actions of neuroglobin include oxygen binding and sensing, scavenging of reactive oxygen and nitrogen species, carbon monoxide sequestration, preservation of mitochondrial homeostasis and brain region- and neuron-type-specific regulatory functions [9–17]. In view of substantive evidence for ameliorative effects of neuroglobin, we produced a genetically modified mouse with neuron-specific overexpression of neuroglobin (Ngb-tg) under the control of synapsin I promoter and assessed the Ngb-tg mouse in a model of acute combustion smoke inhalation [18], which we have developed for the un-anesthetized freely moving mouse [19–21].

We developed the smoke inhalation survival model to facilitate investigation of mechanisms that contribute to adverse sequelae seen in survivors of smoke inhalation incidents, such as occur in enclosed spaces or intense forest fires, who tend to develop lasting neurologic deficits [22–24]. To

Murat F. Gorgun and Ming Zhuo: Co-first authors.

✉ Ella W. Englander
elenglan@utmb.edu

Extended author information available on the last page of the article

this end, we have been studying the smoke-induced temporal molecular, biochemical and cellular changes in the mouse brain and their modulation by neuron specific overexpression of neuroglobin. We observed protection by neuroglobin in vivo, in our mouse model of smoke inhalation [18, 25] and in vitro, in cultured cortical neurons following a nitric oxide challenge [16]. We found that at the early recovery times post-smoke exposure, elevated neuroglobin mitigates mitochondrial impairments, preventing disruption of energy homeostasis and escalation of oxidative stress thereby, lessening formation of oxidative DNA damage in the mouse brain [18], the key factor predicted to contribute to evolution of smoke induced brain injury [18, 25]. Recently, we extended the post-smoke time frame of our studies, to monitor also chronic manifestation including, neurobehavioral impairments and long-term cellular changes in the mouse brain. We found that acute exposure to combustion smoke triggers long-term neuroinflammatory changes, with concordant neurobehavioral deficits in the mouse [26]. In the current study, we demonstrate that elevated neuroglobin exerts long-term neuroprotection in the setting of acute inhalation of combustion smoke.

Materials and Methods

Mouse Model of Acute Inhalation of Combustion Smoke

The parental wild-type CB57BL/6 and transgenic Ngb-tg mouse strains [18] are housed and bred in the Animal Facility at the University of Texas Medical Branch (facility operates in compliance with the USDA Animal Welfare Act, the Guide for the Care and Use of Laboratory Animals, under OLAW accreditation, and IACUC approved protocols). The smoke-inhalation survival model, which we have developed for the un-anesthetized mouse was used [18–21, 25, 27]. At the initial stages of model development, comparisons of smoke exposure outcomes did not reveal gender dependent differences and here we report results obtained with male mice. Briefly, smoke is produced in smoke-generating chamber by smoldering aspen wood shavings (1.3 g/min) and dispersed by a tube-mounted fan into a 20-L transparent mouse exposure chamber. Smoke composition in exposure chamber was 3500 ppm carbon monoxide (0.35%), 11,500 ppm (1.15%) carbon dioxide, 14.5% oxygen and various volatile organic compounds as we reported [20]. Wild-type and Ngb-tg male mice (3–4 months old) were placed in the smoke exposure chamber for 60 min with 10–20 s venting breaks to ambient air at approximately 10-min intervals. Total exposure time had been calibrated to achieve survival rate greater than 95%. Mice handled identically, except for the omission of smoke, served as sham-controls. Venous blood hemodynamic parameters were 5% and 62% carboxyhemoglobin in sham-controls and post-smoke mice, respectively, with a drop to 11% after 2-h post-smoke recovery in ambient air, as we reported [18]. Mice were maintained for 8 months after smoke exposure prior to euthanasia and tissue collection. Mice were evaluated weekly for general health parameters including food intake, weight gain and locomotion. No overt differences were detected between the sham-control and post-smoke groups. As expected, due to cohort attrition during the 8 months, 1–3 mice were lost per group independently of their assignment to either the smoke-exposed or sham-control groups. Schematic diagram of the sequence of experimental procedures is shown in Fig. 1a, b.

Tissue Collection, Immunohistochemistry and Image Analysis

Eight months post-smoke exposure brain tissues were collected and either dissected and snap frozen or fixed in 10% formalin for immunohistological analyses (n = 4). Fixed brains were paraffin embedded and cut to obtain 5 µm coronal sections through Bregma −3.14 region. Sub-hippocampal regions assessed by immunohistological analyses are demarcated on hematoxylin/eosin stained section through this region (Fig. 1c). For immunostaining analyses, sections were processed by standard procedure and incubated with the following primary antibodies: anti-glial fibrillary acidic protein (GFAP, #AB5804, Millipore, at 1:1000), anti-ionized calcium-binding adapter molecule 1 (Iba-1, #019-19741, Wako-Chem, at 1:400) and anti-myelin basic protein (#AB134018, Abcam, at 1:400). Briefly, sections were incubated with primary antibodies for two hours at

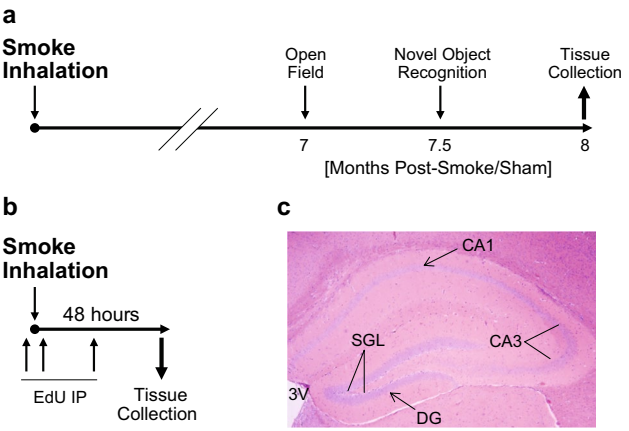

Fig. 1 Schematic diagram of the experimental design. **a**, **b** Timelines of procedures and samples collection. **c** Demarcations of mouse hippocampal regions used for immunohistological analyses on H&E stained coronal section through the hippocampus. CA1, CA3—hippocampal subfields Cornu Ammonis 1 & 3; DG—dentate gyrus; SGL—subgranular layer; 3V—third ventricle

RT, followed by 3 × washes with PBS and 30 min incubation with biotinylated secondary antibody (anti-mouse #BA9200 or anti-rabbit #BA1000 at 1:400, Vector Laboratories) followed by washing and 30-min incubation with horseradish peroxidase streptavidin (#SA5004 Vector Laboratories at 1:400). Staining was developed by 3, 3′-diaminobenzidine (DAB) solution (#K3466, DAKO) and counterstained by hematoxylin (#TA060MH, Thermo Scientific). Images were taken using Nikon Eclipse 600 microscope. ROIs were delineated using ImageJ software and Iba-1 and GFAP positive cells counted using ImageJ. Four non-consecutive sections through the hippocampus were scored. Data were expressed as mean ± SEM cell number per millimeter square in delineated ROIs for each experimental group (n = 4). Myelination patterns were assessed by myelin basic protein (MBP) immunoreactivity. For quantification, counter stain was omitted and images were converted to gray scale, setting threshold intensity at 225. The gray scale images were transformed into binary images using the 'make binary' function of ImageJ. Black areas were defined as positive for myelin as previously described [26, 28–30]. Each CA3 region (left and right) was divided into three contiguous areas for scoring and positive area percent was calculated as we described [26]. Twenty-four ROIs were scored per group (n = 4); data are presented as mean ± SEM percent of area positive for MBP.

Real-Time qPCR

Hippocampal RNA was extracted from snap frozen tissues (n = 3) using the RNeasy plus mini kit (Qiagen, Valencia, CA) as we described [25, 26, 31]. T100 thermal cycler (Biorad) was used to reverse transcribe one microgram of total RNA using the iScript RT supermix (Biorad) that includes random, as well as, oligo dT primers. Real-time PCR reactions were assembled with SSO FAST Evagreen supermix (Bio-Rad) and run using the CFX96 Real-Time System (Biorad). Amplification parameters were 95 °C 2 min, 40 cycles of 95 °C 5 s, 55 °C 15 s with 18S ribosomal RNA gene as reference gene. The relative amount of target gene RNA was calculated according to Schmittgen and Livak [32] using the formula: $-\Delta\Delta Ct = [(CT \text{ gene of interest-CT internal control}) \text{ sample-}(CT \text{ gene of interest-CT internal control}) \text{ control}]$. Primer sequences are provided in Table 1. Data are presented as mean ± SEM (n = 3).

Hippocampal Neurogenesis

Neuronal progenitor cells were detected by incorporation of 5-ethynyl-2′-deoxyuridine (EdU)into genomic DNA of neuronal progenitor cells. EdU was delivered intra peritoneally (IP) by three injections at 50 mg/kg. First injection was given 4 h prior to smoke exposure, followed by second injection 4 h after smoke and third injection 24 h ahead of euthanasia at 48 h post-smoke. Leica, #CM3050 cryostat was used to cut 10 µm hippocampal cryosections. Cryosections were mounted on superfrost plus slides (Fisher #12-550-15), fixed in 10% buffered formalin (Fisher, #SF100-4), permeabilized and blocked by 0.3% Triton-X-100/10% goat serum in citrate buffer for 45 min. Click-iT™ EdU Alexa Fluor™ 488 Imaging Kit (Invitrogen, #C10337) was used to detect EdU incorporation according to manufacturer's protocol as previously described Jao et al. [33] and as we reported [31]. Cover slips were mounted with diamond anti-fade mountant with DAPI (Thermo, #P36962). EdU fluorescence (green) was observed with Olympus IX71 fluorescence microscope. EdU positive cells in the left and right dentate gyrus regions (ROIs) were scored for every tenth section for four sections per mouse (n = 3); 24 ROIs were scored per group. Data are reported as mean ± SEM percent change for total number of EdU positive cells for the post-smoke versus sham control groups.

Neurobehavioral Testing

Neurobehavioral testing was done at the UTMB Rodent In Vivo Assessment Core Facility using standard validated

Table 1 IDs and sequences and of primers used in study

Gene symbol	Sequence		Accession #
	Forward	Reverse	
18S	gtaacccgttgaaccccatt	ccatccaatcggtagtagcg	NR_003278.3, 18S ribosomal RNA
CCL2	catccacgtgttggctca	gatcatcttgctggtgaatgagt	NM_011333.3 chemokine (C–C motif) ligand 2 (Ccl2)
GFAP	acagactttctccaacctccag	ccttctgacacggatttggt	NM_010277.3 glial fibrillary acidic protein
HMOX1	gtcaagcacagggtgacaga	atcacctgcagctcctcaaa	NM_010442 heme oxygenase 1
IFNG	atctggaggaactggcaaaa	ttcaagacttcaaagagtctgagg	NM_008337.4 interferon gamma (Ifng)
IL6	gaggataccactcccaacagac	aagtgcatcatcgttgttcatac	NM_031168.1 interleukin 6 (Il6)
IL12B	ttgctggtgtctccactcat	gggagtccagtccacctcta	NM_001303244.1 interleukin 12b (Il12b)
NOS2	ctttgccacggacgagac	tcattgtactctgagggctgac	NM_010927.3 nitric oxide synthase 2, inducible (Nos2)
TNFA	gcctcttctcattcctgcttg	ctgatgagagggaggccatt	NM_013693.3 tumor necrosis factor (Tnf), variant 1

protocols as we described [26, 33–36]. All testing was done within the 12-h light cycle for return to home cages prior to the 12-h dark cycle. Open field: Mice were acclimated for 60 min in advance of testing. Four opaque wall 38 × 38 cm boxes were simultaneously recorded using the TopScan (Clever Systems Inc) software, which permits demarcation of the chamber's central (12.4 × 12.4 cm) and peripheral arenas. Testing was done seven months post -smoke exposure. Each mouse was placed in the box center and movement was recorded for 10 min using the video tracking system with automated analysis software that quantifies locomotor parameters and dissects distances traveled in periphery and center arena. Boxes were cleaned between tests (70% ethanol) to remove any substances or scents [37]. Open field performance parameters of smoke exposed versus sham control groups for wild-type and Ngb-tg mice (4 groups; n = 8–12) were analyzed by two-tailed t-test or one-way ANOVA followed by Sidak's multiple comparisons test.

Novel Object Recognition (NOR) Test

Sham controls and smoke exposed wild-type and Ngb-tg mice (four groups; n = 8–12) were subjected to learning/memory assessments at 7.5 months post-smoke exposure. Testing was carried out according to standard validated protocols [33–36, 37–40] consisting of training sessions in which the mouse is allowed to explore two identical objects, and testing sessions where one of the original objects is replaced with a novel object, using the intermediate 4-h trial interval [36, 38, 40, 41]. Briefly, mice were habituated by exploration of an empty box for 10-min sessions over two consecutive days. On the third day each mouse was habituated in an empty novel object recognition box for 10 min. Twenty-four hours after the last habituation session mice were subjected to the training session as follows: each mouse was gently placed in a box with two identical objects, with nose facing the middle point of the wall away from objects and let explore for 10 min prior to return to home cage. After a 4-h retention interval, one of the objects was replaced with a novel object and the mouse was placed in a similar manner in the arena for the testing 10-min exploration session. Time spent with the familiar and novel objects during testing was recorded using TopScan digital video-based data capture and analyzed by Topscan version-2 software (CleverSys. Inc). The object discrimination ratio for the testing session was calculated for each mouse using the following formula: *time exploring specified object/(time exploring novel object + time exploring familiar object)* as we described [36, 38, 40, 41]; data are presented as the mean ± SEM. One-sample t-test was used to determine if discrimination ratio was different than chance (0.5) and one-way ANOVA to determine the effect of treatment.

Statistical Analysis

All data are reported as mean ± standard error of the mean (SEM). Two-tailed Student-t test or one-way analysis of variance (ANOVA) followed by Sidak's multiple comparison test was used to analyze differences between the groups. Data were analyzed using Excel or GraphPad Prism software. Statistical significance was determined using a P value ≤ 0.05.

Results

Elevated Neuroglobin Attenuates Long-Term Neuroinflammation and Myelin Depletion Induced in Mouse Hippocampus by Acute Inhalation of Combustion Smoke

We previously found that acute inhalation of combustion smoke induces long-term inflammatory changes in the mouse hippocampus [26]. The changes involve increases in the number of GFAP and Iba-1 positive cells, as well as reduced density of myelinated fibers, suggestive of an onset of a chronic inflammatory condition in the aftermath of acute smoke exposure. In the current study, we found that smoke-induced inflammatory changes are averted in brains of Ngb-tg mice when compared to the smoke exposed wild-type mice. Astrocytes and microglia in the CA1 and dentate gyrus hippocampal regions were assessed by immunoreactivity of the astrocytic glial fibrillary acidic protein (GFAP) and the microglial marker, ionized calcium binding protein (Iba-1), respectively [42, 43], whereas myelination patterns were evaluated by immunoreactivity of myelin basic protein (MBP), a major structural protein in myelin sheath [44]. By 8 months after smoke exposure, no significant increases in the number of GFAP and Iba-1 positive cells were observed in the Ngb-tg brains, when compared sham controls. In contrast, post-smoke analyses revealed increases in numbers of GFAP and Iba-1 positive cells in the similarly exposed wild-type mice (Figs. 2, 3, and Table 2). Likewise, density of myelinated fibers assessed by MBP immunoreactivity (Fig. 4) was reduced by smoke exposure in the wild-type but remained unchanged in hippocampi of Ngb-tg mice. For quantification of myelinated fibers, counter staining with hematoxylin was omitted and MBP immunoreactivity was transformed into binary gray scale images. Quantification revealed reduced post-smoke MBP density in CA3 regions of wild-type but not Ngb-tg mice. In combination, immunohistochemical analyses demonstrated that long-term inflammatory changes that manifest after smoke inhalation in wild-type brains are alleviated in brains of the similarly treated Ngb-tg transgenic mice.

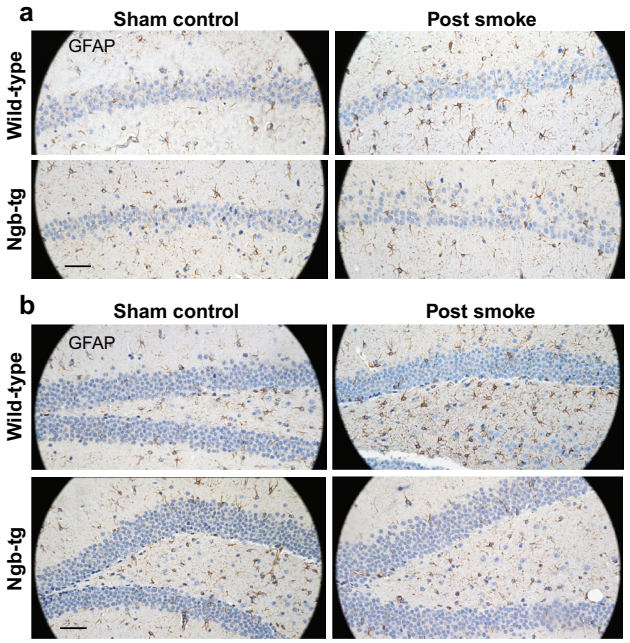

Fig. 2 Increased numbers of GFAP positive cells in CA1 and dentate gyrus regions of wild-type but not Ngb-tg mice analyzed eight months after acute inhalation of smoke. Representative images of GFAP staining in CA1 (**a**) and dentate gyrus (**b**) of sham-controls (left) and post-smoke (right), wild-type (top panels) and Ngb-tg (bottom panels) mice (nuclei stain blue with hematoxylin; scale bar = 50 µm). Quantitation of GFAP positive cell number/mm^2 in ROI is given as mean ± SEM in Table 2. $P < 0.05$ was considered significant (experimental group n = 4)

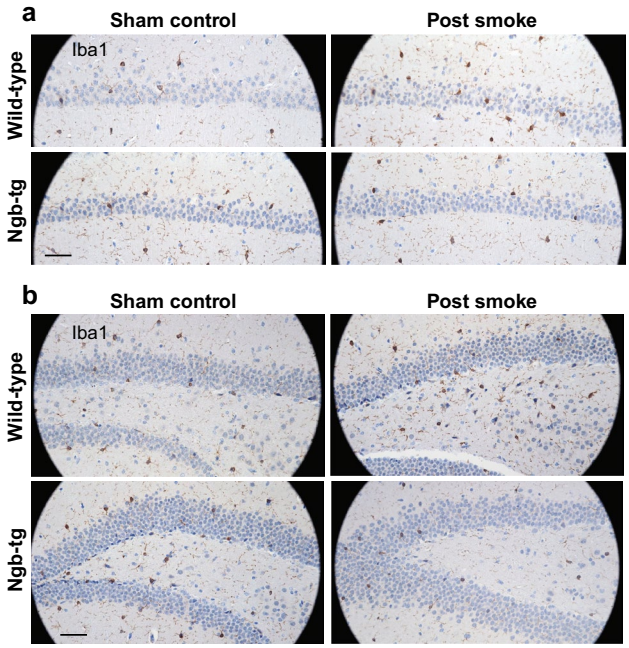

Fig. 3 Increased numbers of Iba-1 positive cells in CA1 and dentate gyrus regions of wild-type but not Ngb-tg mice is observed eight months after acute inhalation of smoke. Representative images of Iba-1 positive microglia in CA1 (**a**) and DG (**b**) of sham-controls (left) and post-smoke (right), wild-type (top panels) and Ngb-tg (bottom panels) mice (hematoxylin counter stain; scale bar = 50 µm). Quantitation of Iba-1 positive cell number/mm^2 in ROI is given as mean ± SEM in Table 2. $P < 0.05$ was considered significant (experimental group n = 4)

Smoke Induced Changes in Inflammatory Gene Expression are Attenuated in the Ngb-Tg Mouse

The extent of changes in mRNAs levels of proinflammatory cytokines post-smoke exposure was compared in hippocampi of wild-type and Ngb-tg mice. RNA extracted from hippocampai of mice maintained eight months post-smoke and age matched sham controls was probed for expression of genes associated with inflammatory processes [45]. Elevated levels of mRNAs for glial fibrillary acidic protein (GFAP), interleukin-12 beta (IL-12B), interferon gamma (IFN-γ), tumor necrosis factor-α (TNF-α) and the chemokine C–C motif ligand 2 (CCL2), as well as, elevated expression of heme oxygenase 1 (HMOX1), a phase ll antioxidant enzyme, were detected (Fig. 5). Comparison of the extent of change in gene expression induced by smoke in the wild-type and in the Ngb-tg mice revealed a trend for attenuation of the smoke-induced upregulation of inflammatory gene expression in the Ngb-tg hippocampus. Most of the analyzed genes were significantly less upregulated in Ngb-tg hippocampi when compared to the similarly exposed wild-type mice, consistent with the possibility that neuroglobin contributes to preservation of anti-inflammatory environment [5].

Post-smoke Reduction in Neurogenesis in Subgranular Zone of the Dentate Gyrus of Wild-Type and Ngb-tg Mice is Comparable

Conditions that adversely affect the brain have been implicated in impediment of adult neurogenesis [46, 47]. Here, the status of post-smoke neurogenesis in subgranular layer of dentate gyrus was assessed by incorporation of the thymidine analog, EdU, into newly synthesized genomic DNA of neuronal progenitor cells that divide prior to their differentiation into neurons. We found that by 48 h after acute smoke exposure, hippocampal neurogenesis was significantly reduced in both the wild-type, as well as Ngb-tg mice (Fig. 6). Because the Ngb-tg mouse is engineered to overexpress neuroglobin under the control of synapsin l promoter [18], overexpression is limited to differentiated neurons that express synapsin l [48]. Accordingly, effects of elevated neuroglobin on neurogenesis are not directly testable in this transgenic model. Rather our findings are consistent with the substantive evidence showing protection by neuroglobin of mature neurons in diverse models of neuronal injury [5, 6, 10]. These findings indicate that

Table 2 Post smoke changes in density of GFAP and Iba-1 positive cells in CA1 and dentate gyrus regions

	Wild-type		Ngb-tg	
	Sham control	Post smoke	Sham control	Post smoke
$GFAP^+$ cells/mm^2				
CA1	153 ± 14	191 ± 10*	169 ± 12	153 ± 9
Dentate gyrus	384 ± 19	450 ± 13*	400 ± 39	411 ± 5
Iba-1^+ cells/mm^2				
CA1	86 ± 4	130 ± 8*	100 ± 6	67 ± 5*
Dentate gyrus	100 ± 16	145 ± 8*	100 ± 5	111 ± 12

Values are mean ± SEM; *$P < 0.05$ post smoke versus sham control

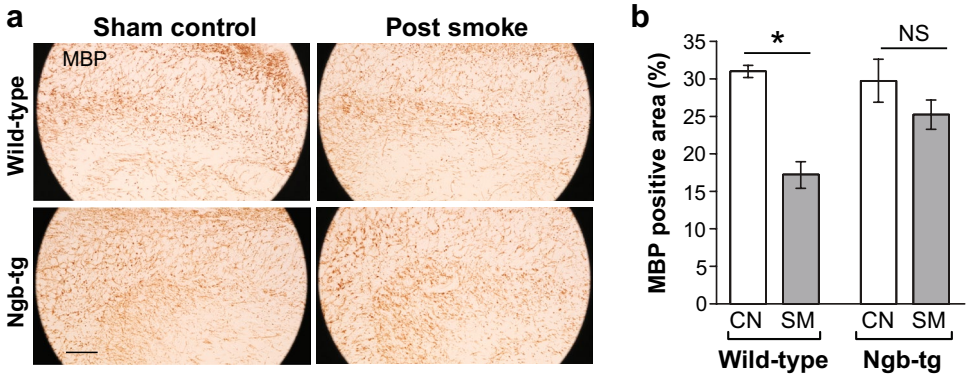

Fig. 4 Myelin basic protein (MBP) immunoreactivity is reduced after acute inhalation of smoke in CA3 hippocampal regions of wild-type but not Ngb-tg mice. **a** Representative images of coronal sections immunostained for MBP are shown. For quantification purposes, sections were immunostained for MBP without hematoxylin counterstain. Images were converted to gray scale and assigned positivity threshold; images of CA3 regions generated by the 'make binary function' of ImageJ were analyzed. **b** Bar graphs show mean ± SEM percent for MBP positive areas calculated from 24 regions of interest scored per each of the four experimental groups: sham controls (CN) and post-smoke (SM) wild-type and Ngb-tg mice (n = 4); *$P < 0.05$; *NS* not significant

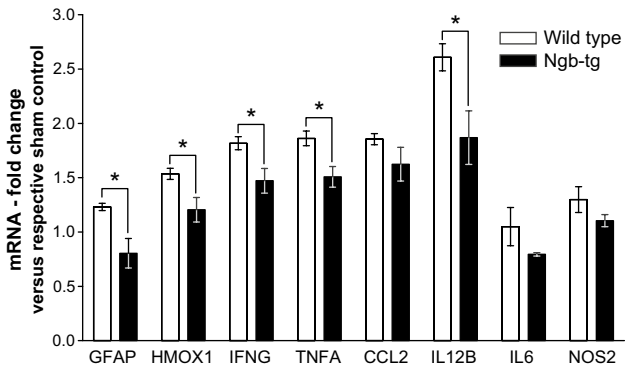

Fig. 5 Post-smoke hippocampal inflammatory gene expression is elevated to a greater extent in wild-type compared to Ngb-tg mice. Real time-qPCR revealed higher mRNA levels of inflammatory genes in post-smoke hippocampi of wild-type when compared to Ngb-tg mice. Data are presented as mean ± SEM of expression fold change versus the respective sham controls (n = 3); *Indicates different from smoke-induced fold change in the wild-type mouse (GFAP p = 0.0461; IL-12B p = 0.0265; IFN-γ p = 0.0202; TNF-α p = 0.0264; HMOX1 p = 0.0291)

in our model neuroglobin exerts protection via mechanisms other than direct modulation of neurogenesis.

Elevated Neuroglobin Mitigates Long-Term Neurobehavioral Deficits Induced in Mice by Acute Inhalation of Combustion Smoke

In view of attenuated inflammatory changes in the Ngb-tg brains, we asked whether neuroglobin might mitigate also the smoke induced neurobehavioral deficits observed in longitudinal studies with the smoke exposed wild-type mice [26]. In the current study, wild-type and Ngb-tg mice were evaluated in Open Field (OF) and New Object Recognition (NOR) testing paradigms. OF testing gauges the mouse locomotor performance and exploratory behavior [34, 35, 37], whereas NOR testing serves to assess learning and memory functions [35, 36, 38, 40]. We subjected Ngb-tg and wild-type mice to OF testing at seven months post-acute exposure to combustion smoke. Locomotion

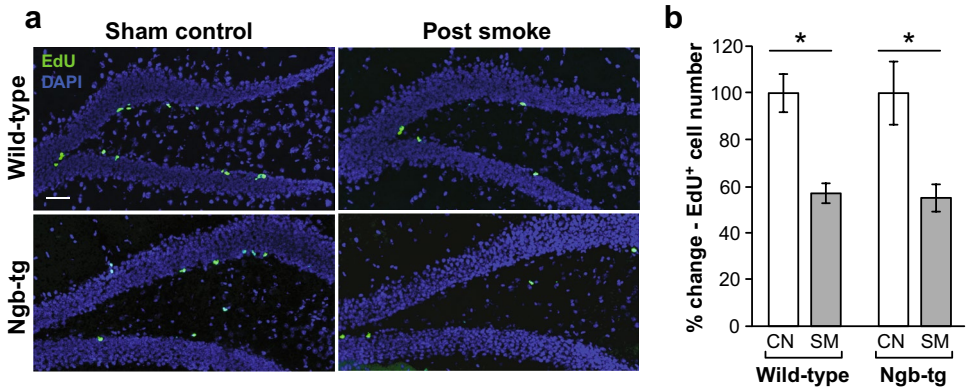

Fig. 6 Smoke exposures reduce adult neurogenesis in the mouse dentate gyrus. Neurogenesis was monitored by incorporation of EdU, a traceable thymidine analog, into newly synthesized DNA of neuronal progenitor cells in the subgranular zone of dentate gyrus. **a** Representative merged images of EdU/DAPI staining are shown for sham-controls (left) and post-smoke (right) wild-type (top) and Ngb-tg (bottom) mice, depicting EdU incorporation (green) into nuclear DNA of neuronal progenitors (nuclei stain blue with DAPI; scale bar = 50 µm). **b** Quantitation of EdU positive cells 48 h after smoke (SM) and sham (CN) exposures; data are expressed as mean ± SEM percent change relative to respective sham-control in EdU positive cells in subgranular zone of dentate gyrus (n = 3 mice) $^*P < 0.05$

patterns and distances traveled were recorded for wild-type and Ngb-tg sham-controls, as well as, the wild-type and Ngb-tg post-smoke groups (n = 8–12). Recording was done using the TopScan video tracking system and automated software (Fig. 7). When compared to the respective sham-controls, analyses revealed a ~ 20% reduction in

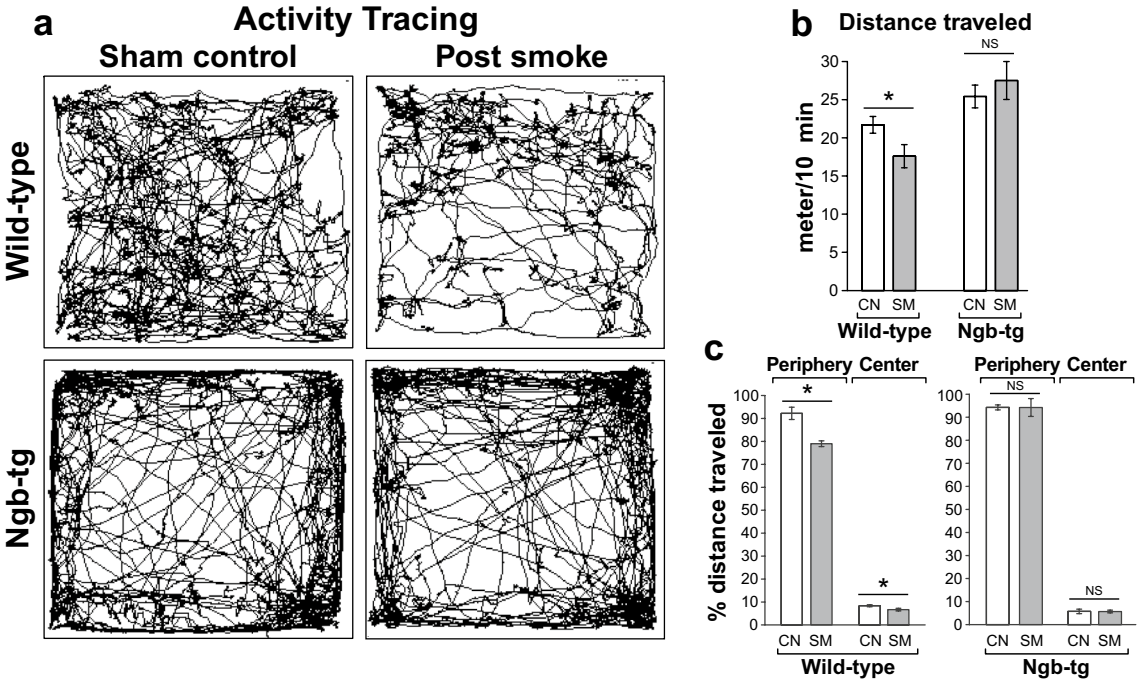

Fig. 7 Smoke exposed wild-type but not Ngb-tg mice exhibit anxiety-like behavior. Testing in Open Field revealed reduced total distance traveled and avoidance of central arena in the wild-type mice seven months post-smoke exposure. **a** Representative images of movement traces recorded simultaneously in four test boxes representing the four different test groups: sham-controls (left), post-smoke (right), wild-type (top), Ngb-tg (bottom). **b** Analysis of the total traveled distance revealed reduced distance in smoke exposed (SM) compared to sham-control (CN) wild-type mice, but not in the smoke exposed Ngb-tg mice. Data are presented as mean ± SEM of total distance traveled. **c** Relative distance traveled in the periphery and in the central arena was reduced in the post-smoke compared to sham-control wild-type mice ($P = 0.0148$ and $P = 0.0312$, respectively), but not in post-smoke Ngb-tg mice. Data are presented as mean ± SEM of relative distance traveled; $^*P < 0.05$; *NS* not significant

total distance traveled in smoke exposed wild-type but not the smoke-exposed Ngb-tg mice (Fig. 7b). Notably, activity traces also revealed reduced exploration of the center arena suggestive of anxiety-like behavior in the post-smoke wild-type but not post-smoke Ngb-tg (Fig. 7c). The results for the wild-type mice are in agreement with our earlier findings using additional testing paradigms, which revealed persistent anxiety-like behavior in wild-type mice following acute smoke exposure [26]. Here, we expanded the scope of testing and asked whether acute exposure to smoke could also affect learning and memory functions. The new object recognition (NOR) paradigm [36, 38, 40], which exploits rodent's ability to distinguish previously explored from novel objects was chosen for testing. We found that after acute smoke exposure, the discrimination ratio between novel and familiar objects was reduced in the wild-type but not in Ngb-tg mice (Fig. 8), indicating that in Ngb-tg, protection by elevated neuroglobin of targets adversely affected by smoke inhalation prevents also the development of memory deficits.

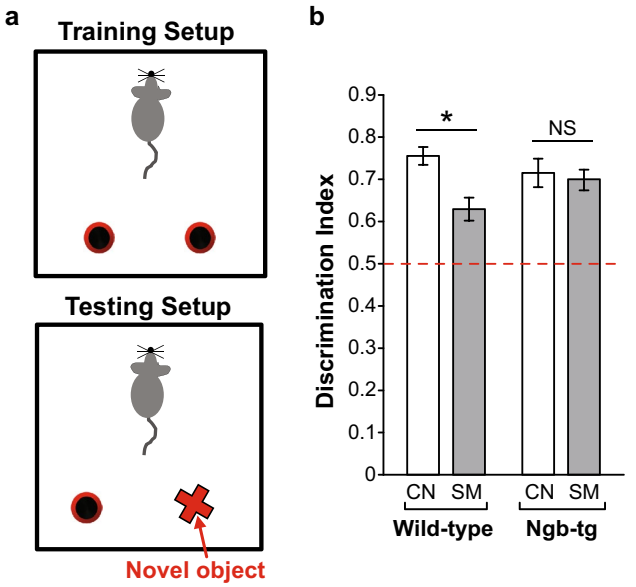

Fig. 8 Novel Object Recognition (NOR) testing post-smoke revealed a memory deficit in wild-type but not in Ngb-tg mice. **a** Graphic representation of the NOR training and testing setup. **b** Discrimination ratio between novel and familiar object was significantly reduced after smoke exposure in the wild-type (0.629 ± 0.027 versus 0.755 ± 0.021) but not in Ngb-tg mice when compared to the respective sham-controls (0.699 ± 0.023 versus 0.715 ± 0.034). Data are presented as discrimination index mean ± SEM. Two-tailed Student-t test was used to compare between sham control (CN) and smoke-exposed (SM) mice; $^*P < 0.05$ was considered significant; *NS* not significant

Discussion

Acute inhalation of combustion smoke, such as may occur in house fires and other enclosed spaces, leads to early as well as delayed neurological sequelae in survivors [22, 23, 48–51]. The primary neurotoxic components of smoke include carbon monoxide, hydrogen cyanide and organic volatile compounds that synergize with hypoxia and free radical-generators to initiate brain injury [51–54]. To date, unlike the better characterized sequelae of carbon monoxide poisoning [54–60], the progression of chronic neurological deficits resulting from acute inhalation of smoke remains understudied. Consequently, the mechanistic link between smoke-induced perturbation of brain homeostasis and onset of delayed neurological consequences is not well understood [60–63] and the question as to whether akin to other types of brain injury, acute exposure to combustion smoke might predispose to brain disorders later in life is still open.

To address these issues, we have developed a long-term survival smoke-inhalation model for the un-anesthetized, freely moving mouse [26]. Our earlier studies in this model that focused on short-term post-smoke recovery times revealed mitochondrial perturbations, reduced ATP levels and formation of oxidative DNA damage in the mouse brain [19–21, 27], whereas assessments at long-term post-smoke recovery times, revealed neuroinflammatory changes and neurobehavioral deficits [26]. We produced a transgenic mouse (Ngb-tg) with neuron-specific overexpression of neuroglobin [18], an oxygen binding neuronal protein that proved protective in many different models of hypoxic and ischemic brain injuries [13, 17, 63–66], as well as models of neurodegenerative disease [66–70]. Using the Ngb-tg mouse, we reported that at the early recovery times elevated neuroglobin helps sustain mitochondrial respiration and ATP content, raising the threshold of smoke injury in the brain [18, 25], and in vitro, raising the threshold of nitric oxide injury in primary cortical neurons [16]. In the current study, to assess the potential role of elevated neuroglobin in long-term neuroprotection, manifestations of acute smoke exposure were compared in the wild-type and Ngb-tg mice. We found that elevated neuroglobin attenuates inflammatory changes induced in the brain by smoke exposure and alleviates concomitant long-term neurobehavioral deficits. Specifically, elevated neuroglobin attenuated the post-smoke increases in inflammatory cytokine expression, in the numbers of GFAP and Iba-1 positive cells and depletion of myelin in hippocampal regions of the Ngb-tg mouse brain. Importantly, neuroglobin alleviated the smoke inhalation-induced learning/memory deficit that developed in wild-type mice after acute inhalation of combustion smoke.

Although, we still lack a unifying mechanism to account for the neuroglobin mediated protection reported

in many settings of brain injury, the extant literature cites many outcome measures that are highly relevant to smoke-induced perturbations of neuronal function. The reported protective effects of neuroglobin span cytosolic and mitochondrial compartments and include temporary oxygen storage under hypoxic conditions, neutralization of reactive oxygen and nitrogen species, sequestration of carbon monoxide, augmentation of the electron transfer chain [9, 10, 14, 15], trapping of catecholamine oxidation products [71], G-protein modulation that averts apoptosis and favors neuronal survival [72, 73] and regulation of neuronal energy metabolism [74]. In view of neuroglobin-mediated protection of many targets that are perturbed by smoke exposures [18, 25], we hypothesized that the magnitude of adverse long-term manifestations of smoke, might also be reduced, due at least in part, to anti-inflammatory milieu maintained by elevated neuroglobin [5–8]. Interestingly, a therapeutic application based on the high affinity of neuroglobin for carbon monoxide, the major component of smoke, has been developed recently [9]. In that case, investigators modified neuroglobin structure to further augment its binding affinity for carbon monoxide in effort to produce a life-saving antidote for carbon monoxide poisoning [9, 75] that is criticaly pertinent and applicable to combustion smoke exposures.

In addition to the previously observed molecular and cellular changes [19–21, 27], activation of immunoinflammatory pathways by smoke exposure at early recovery times has been reported [76]. While we detected neuroinflammatory changes in the wild-type mouse brain also 8 months after initial smoke esposure [26], no significant neuroinflammatory changes involving astrogliosis, microgliosis or myelin depletion were evident in the Ngb-tg brain. An important aspect of our long-term studies is that ameliorative effects detected at the cellular and tissue level in the post-smoke Ngb-tg brains, are concordant with alleviation of smoke induced neurobehavioral deficits. Using the Open Field testing paradigm, we detected reduced exploratory activity in the wild-type but not in the Ngb-tg mice seven months after exposure to smoke (Fig. 7). The marked avoidance of center arena by the post-smoke wild-type mice is suggestive of anxiety-like behaviour. This is consistent with other anxiety indicators, including reduced time in the open arms of elevated plus maze and increased cued freezing behavior, which we previously observed post-smoke in wild-type mice [26]. Here, using the NOR testing paradigm, long-term impairment in the learning/memory task was detected in wild-type but not Ngb-tg mice subjected to identical smoke exposure (Fig. 8). NOR is a hippocampus- and prefronatal cortex dependent task [77] and this outcome is consistent with preservation of cognitive function in Ngb-tg mice, plausibly due to the anti-inflammatory environment maintained by elevated neuroglobin. Elevated neuroglobin has been previously linked with improvment of neurologic function in aged mice, where age-associated neuroinflammation contributes to neurologic deficits [78].

Of note, in the current study, we found that smoke exposure has an acute inhibitory effect on subgranular zone/dentate gyrus neurogenesis. While it is still unresolved to what extent modulations of adult neurogenesis correlate with neurobehavioral changes [79, 80], adult neurogenesis is considered critical for brain plasticity and its compromise has been associated with neurodegenerative disease [46]. Here we demonstrate for the first time that dentate gyrus neurogenesis is reduced following acute exposure to combustion smoke. However, because the Ngb-tg transgene is under the control of synapsin l promoter, in our system neuroglobin overexpresion is restricted to differentiated neurons and absent from progenitor cells that drive neurogenesis. Hence, while neuroglobin has been previously implicated in promoting neurogenesis [81], due to the transgene design, this particular aspect of neuroglobin is not testable in our experimental system.

Interestingly, while neuroglobin was found protective in many models of brain injury, only few studies have explored the long-term protective effects of neuroglobin, particularly as they pertain to manifestations of neurologic deficits. Our data suggest that preservation of mitochondrial function and energy homeostasis that have been attributed to neuroglobin in many models of brain injury might help mitigate the impact of smoke exposure averting neuropathologic outcomes and progression of neurologic deficits. Our results demonstrate that manipulation of neuroglobin levels might be useful for prevention of adverse effects of smoke inhalation injury and broaden the scope of therapeutic applications of neuroglobin, suggesting that pharmacologic approaches to augment neuroglobin levels following acute smoke exposure warrant further investigation.

Funding This work was supported by grants from Shriners Hospitals for Children (86700) and the National Institutes of Health (ES014613) to EWE.

Compliance with Ethical Standards

Conflict of interest The authors declare that they have no conflict of interest.

References

1. Burmester T, Weich B, Reinhardt S, Hankeln T (2000) A vertebrate globin expressed in the brain. Nature 407:520–523
2. Droge J, Pande A, Englander EW, Makalowski W (2012) Comparative genomics of neuroglobin reveals its early origins. PLoS ONE 7:e47972

3. Hundahl CA, Allen GC, Hannibal J, Kjaer K, Rehfeld JF, Dewilde S, Nyengaard JR, Kelsen J, Hay-Schmidt A (2010) Anatomical characterization of cytoglobin and neuroglobin mRNA and protein expression in the mouse brain. Brain Res 1331:58–73
4. Hundahl CA, Allen GC, Nyengaard JR, Dewilde S, Carter BD, Kelsen J, Hay-Schmidt A (2008) Neuroglobin in the rat brain: localization. Neuroendocrinology 88:173–182
5. Van Acker ZP, Luyckx E, Dewilde S (2019) Neuroglobin expression in the brain: a story of tissue homeostasis preservation. Mol Neurobiol 56:2101–2122
6. Burmester T, Hankeln T (2009) What is the function of neuroglobin? J Exp Biol 212:1423–1428
7. Baez E, Echeverria V, Cabezas R, Avila-Rodriguez M, Garcia-Segura LM, Barreto GE (2016) Protection by neuroglobin expression in brain pathologies. Front Neurol 7:146
8. Guidolin D, Tortorella C, Marcoli M, Maura G, Agnati LF (2016) Neuroglobin, a factor playing for nerve cell survival. Int J Mol Sci 17:1817
9. Azarov I, Wang L, Rose JJ, Xu Q, Huang XN, Belanger A, Wang Y, Guo L, Liu C, Ucer KB, McTiernan CF, O'Donnell CP, Shiva S, Tejero J, Kim-Shapiro DB, Gladwin MT (2016) Five-coordinate H64Q neuroglobin as a ligand-trap antidote for carbon monoxide poisoning. Sci Transl Med 8:368ra173
10. Brittain T, Skommer J (2012) Does a redox cycle provide a mechanism for setting the capacity of neuroglobin to protect cells from apoptosis? IUBMB Life 64:419–422
11. Hundahl CA, Fahrenkrug J, Hay-Schmidt A, Georg B, Faltoft B, Hannibal J (2012) Circadian behaviour in neuroglobin deficient mice. PLoS ONE 7:e34462
12. Hundahl CA, Kelsen J, Dewilde S, Hay-Schmidt A (2008) Neuroglobin in the rat brain (II): co-localisation with neurotransmitters. Neuroendocrinology 88:183–198
13. Khan AA, Wang Y, Sun Y, Mao XO, Xie L, Miles E, Graboski J, Chen S, Ellerby LM, Jin K, Greenberg DA (2006) Neuroglobin-overexpressing transgenic mice are resistant to cerebral and myocardial ischemia. Proc Natl Acad Sci USA 103:17944–17948
14. Kiger L, Tilleman L, Geuens E, Hoogewijs D, Lechauve C, Moens L, Dewilde S, Marden MC (2011) Electron transfer function versus oxygen delivery: a comparative study for several hexacoordinated globins across the animal kingdom. PLoS ONE 6:e20478
15. Li W, Wu Y, Ren C, Lu Y, Gao Y, Zheng X, Zhang C (2011) The activity of recombinant human neuroglobin as an antioxidant and free radical scavenger. Proteins 79:115–125
16. Singh S, Zhuo M, Gorgun FM, Englander EW (2013) Overexpressed neuroglobin raises threshold for nitric oxide-induced impairment of mitochondrial respiratory activities and stress signaling in primary cortical neurons. Nitric Oxide 32:21–28
17. Sun Y, Jin K, Peel A, Mao XO, Xie L, Greenberg DA (2003) Neuroglobin protects the brain from experimental stroke in vivo. Proc Natl Acad Sci USA 100:3497–3500
18. Lee HM, Greeley GH Jr, Englander EW (2011) Transgenic overexpression of neuroglobin attenuates formation of smoke-inhalation-induced oxidative DNA damage, in vivo, in the mouse brain. Free Radic Biol Med 51:2281–2287
19. Lee HM, Greeley GH, Herndon DN, Sinha M, Luxon BA, Englander EW (2005) A rat model of smoke inhalation injury: influence of combustion smoke on gene expression in the brain. Toxicol Appl Pharmacol 208:255–265
20. Lee HM, Hallberg LM, Greeley GH Jr, Englander EW (2010) Differential inhibition of mitochondrial respiratory complexes by inhalation of combustion smoke and carbon monoxide, in vivo, in the rat brain. Inhal Toxicol 22:770–777
21. Lee HM, Reed J, Greeley GH Jr, Englander EW (2009) Impaired mitochondrial respiration and protein nitration in the rat hippocampus after acute inhalation of combustion smoke. Toxicol Appl Pharmacol 235:208–215
22. Hartzell GE (1996) Overview of combustion toxicology. Toxicology 115:7–23
23. Rossi J 3rd, Ritchie GD, Macys DA, Still KR (1996) An overview of the development, validation, and application of neurobehavioral and neuromolecular toxicity assessment batteries: potential applications to combustion toxicology. Toxicology 115:107–117
24. Stefanidou M, Athanaselis S, Spiliopoulou C (2008) Health impacts of fire smoke inhalation. Inhal Toxicol 20:761–766
25. Gorgun FM, Zhuo M, Singh S, Englander EW (2014) Neuroglobin mitigates mitochondrial impairments induced by acute inhalation of combustion smoke in the mouse brain. Inhal Toxicol 26:361–369
26. Gorgun MF, Zhuo M, Cortez I, Dineley KT, Englander EW (2017) Acute inhalation of combustion smoke triggers neuroinflammation and persistent anxiety-like behavior in the mouse. Inhal Toxicol 29:598–610
27. Chen L, Lee HM, Greeley GH Jr, Englander EW (2007) Accumulation of oxidatively generated DNA damage in the brain: a mechanism of neurotoxicity. Free Radic Biol Med 42:385–393
28. Hammelrath L, Skokic S, Khmelinskii A, Hess A, van der Knaap N, Staring M, Lelieveldt BPF, Wiedermann D, Hoehn M (2016) Morphological maturation of the mouse brain: an in vivo MRI and histology investigation. Neuroimage 125:144–152
29. Tu TW, Kim JH, Yin FQ, Jakeman LB, Song SK (2013) The impact of myelination on axon sparing and locomotor function recovery in spinal cord injury assessed using diffusion tensor imaging. NMR Biomed 26:1484–1495
30. Zhang H, Yan G, Xu H, Fang Z, Zhang J, Zhang J, Wu R, Kong J, Huang Q (2016) The recovery trajectory of adolescent social defeat stress-induced behavioral, (1)H-MRS metabolites and myelin changes in Balb/c mice. Sci Rep 6:27906
31. Zhuo M, Gorgun MF, Englander EW (2018) Translesion synthesis DNA polymerase kappa is indispensable for DNA repair synthesis in cisplatin exposed dorsal root ganglion neurons. Mol Neurobiol 55:2506–2515
32. Schmittgen TD, Livak KJ (2008) Analyzing real-time PCR data by the comparative C(T) method. Nat Protoc 3:1101–1108
33. Jao CY, Salic A (2008) Exploring RNA transcription and turnover in vivo by using click chemistry. Proc Natl Acad Sci U S A 105:15779-15784
34. Dineley KT, Hogan D, Zhang WR, Taglialatela G (2007) Acute inhibition of calcineurin restores associative learning and memory in Tg2576 APP transgenic mice. Neurobiol Learn Mem 88:217–224
35. Dineley KT, Xia X, Bui D, Sweatt JD, Zheng H (2002) Accelerated plaque accumulation, associative learning deficits, and up-regulation of alpha 7 nicotinic receptor protein in transgenic mice co-expressing mutant human presenilin 1 and amyloid precursor proteins. J Biol Chem 277:22768–22780
36. Taglialatela G, Hogan D, Zhang WR, Dineley KT (2009) Intermediate- and long-term recognition memory deficits in Tg2576 mice are reversed with acute calcineurin inhibition. Behav Brain Res 200:95–99
37. Crawley JN, Paylor R (1997) A proposed test battery and constellations of specific behavioral paradigms to investigate the behavioral phenotypes of transgenic and knockout mice. Horm Behav 31:197–211
38. Bevins RA, Besheer J (2006) Object recognition in rats and mice: a one-trial non-matching-to-sample learning task to study 'recognition memory'. Nat Protoc 1:1306–1311
39. Hernandez CM, Kayed R, Zheng H, Sweatt JD, Dineley KT (2010) Loss of alpha7 nicotinic receptors enhances beta-amyloid oligomer accumulation, exacerbating early-stage cognitive decline and septohippocampal pathology in a mouse model of Alzheimer's disease. J Neurosci 30:2442–2453

40. Leger M, Quiedeville A, Bouet V, Haelewyn B, Boulouard M, Schumann-Bard P, Freret T (2013) Object recognition test in mice. Nat Protoc 8:2531–2537
41. Pavlopoulos E, Jones S, Kosmidis S, Close M, Kim C, Kovalerchik O, Small SA, Kandel ER (2013) Molecular mechanism for age-related memory loss: the histone-binding protein RbAp48. Sci Transl Med 5:200ra115
42. Prokop S, Miller KR, Heppner FL (2013) Microglia actions in Alzheimer's disease. Acta Neuropathol 126:461–477
43. Xu H, Zhang SL, Tan GW, Zhu HW, Huang CQ, Zhang FF, Wang ZX (2012) Reactive gliosis and neuroinflammation in rats with communicating hydrocephalus. Neuroscience 218:317–325
44. Schregel K, Wuerfel E, Garteiser P, Gemeinhardt I, Prozorovski T, Aktas O, Merz H, Petersen D, Wuerfel J, Sinkus R (2012) Demyelination reduces brain parenchymal stiffness quantified in vivo by magnetic resonance elastography. Proc Natl Acad Sci USA 109:6650–6655
45. Becher B, Spath S, Goverman J (2017) Cytokine networks in neuroinflammation. Nat Rev Immunol 17:49–59
46. Moreno-Jimenez EP, Flor-Garcia M, Terreros-Roncal J, Rabano A, Cafini F, Pallas-Bazarra N, Avila J, Llorens-Martin M (2019) Adult hippocampal neurogenesis is abundant in neurologically healthy subjects and drops sharply in patients with Alzheimer's disease. Nat Med 25:554–560
47. Zywitza V, Misios A, Bunatyan L, Willnow TE, Rajewsky N (2018) Single-cell transcriptomics characterizes cell types in the subventricular zone and uncovers molecular defects impairing adult neurogenesis. Cell Rep 25:2457–2469
48. Pieribone VA, Porton B, Rendon B, Feng J, Greengard P, Kao HT (2002) Expression of synapsin III in nerve terminals and neurogenic regions of the adult brain. J Comp Neurol 454:105–114
49. Alarie Y (2002) Toxicity of fire smoke. Crit Rev Toxicol 32:259–289
50. Smith SM, Stuhmiller JH, Januszkiewicz AJ (1996) Evaluation of lethality estimates for combustion gases in military scenarios. Toxicology 115:157–165
51. Stuhmiller JH, Long DW, Stuhmiller LM (2006) An internal dose model of incapacitation and lethality risk from inhalation of fire gases. Inhal Toxicol 18:347–364
52. Baud F, Boukobza M, Borron SW (2011) Cyanide: an unreported cause of neurological complications following smoke inhalation. BMJ Case Rep. https://doi.org/10.1136/bcr.09.2011.4881
53. Dries DJ, Endorf FW (2013) Inhalation injury: epidemiology, pathology, treatment strategies. Scand J Trauma Resusc Emerg Med 21:31
54. Geldner G, Koch EM, Gottwald-Hostalek U, Baud F, Burillo G, Fauville JP, Levi F, Locatelli C, Zilker T (2013) Report on a study of fires with smoke gas development: determination of blood cyanide levels, clinical signs and laboratory values in victims. Anaesthesist 62:609–616
55. Huang CC, Chung MH, Weng SF, Chien CC, Lin SJ, Lin HJ, Guo HR, Su SB, Hsu CC, Juan CW (2014) Long-term prognosis of patients with carbon monoxide poisoning: a nationwide cohort study. PLoS ONE 9:e105503
56. Mizuno Y, Sakurai Y, Sugimoto I, Ichinose K, Ishihara S, Sanjo N, Mizusawa H, Mannen T (2014) Delayed leukoencephalopathy after carbon monoxide poisoning presenting as subacute dementia. Intern Med 53:1441–1445
57. Pages B, Planton M, Buys S, Lemesle B, Birmes P, Barbeau EJ, Maziero S, Cordier L, Cabot C, Puel M, Genestal M, Chollet F, Pariente J (2014) Neuropsychological outcome after carbon monoxide exposure following a storm: a case-control study. BMC Neurol 14:153
58. Pang L, Wang HL, Wang ZH, Wu Y, Dong N, Xu DH, Wang DW, Xu H, Zhang N (2014) Plasma copeptin as a predictor of intoxication severity and delayed neurological sequelae in acute carbon monoxide poisoning. Peptides 59:89–93
59. Tsai CF, Yip PK, Chen SY, Lin JC, Yeh ZT, Kung LY, Wang CY, Fan YM (2014) The impacts of acute carbon monoxide poisoning on the brain: longitudinal clinical and 99mTc ethyl cysteinate brain SPECT characterization of patients with persistent and delayed neurological sequelae. Clin Neurol Neurosurg 119:21–27
60. Yeh ZT, Tsai CF, Yip PK, Lo CY, Peng SM, Chen SY, Kung LY (2014) Neuropsychological performance in patients with carbon monoxide poisoning. Appl Neuropsychol Adult 21:278–287
61. Anseeuw K, Delvau N, Burillo-Putze G, De Iaco F, Geldner G, Holmstrom P, Lambert Y, Sabbe M (2013) Cyanide poisoning by fire smoke inhalation: a European expert consensus. Eur J Emerg Med 20:2–9
62. Antonio AC, Castro PS, Freire LO (2013) Smoke inhalation injury during enclosed-space fires: an update. J Bras Pneumol 39:373–381
63. Lawson-Smith P, Jansen EC, Hyldegaard O (2011) Cyanide intoxication as part of smoke inhalation–a review on diagnosis and treatment from the emergency perspective. Scand J Trauma Resusc Emerg Med 19:14
64. Chen F, Lu J, Chen F, Lin Z, Lin Y, Yu L, Su X, Yao P, Cai B, Kang D (2018) Recombinant neuroglobin ameliorates early brain injury after subarachnoid hemorrhage via inhibiting the activation of mitochondria apoptotic pathway. Neurochem Int 112:219–226
65. Xiong XX, Pan F, Chen RQ, Hu DX, Qiu XY, Li CY, Xie XQ, Tian B, Chen XQ (2018) Neuroglobin boosts axon regeneration during ischemic reperfusion via p38 binding and activation depending on oxygen signal. Cell Death Dis 9:163
66. Zhang B, Ji X, Zhang S, Ren H, Wang M, Guo C, Li Y (2013) Heminmediated neuroglobin induction exerts neuroprotection following ischemic brain injury through PI3K/Akt signaling. Mol Med Rep 8:681–685
67. Chen LM, Xiong YS, Kong FL, Qu M, Wang Q, Chen XQ, Wang JZ, Zhu LQ (2012) Neuroglobin attenuates Alzheimer-like tau hyperphosphorylation by activating Akt signaling. J Neurochem 120:157–164
68. Khan AA, Mao XO, Banwait S, Jin K, Greenberg DA (2007) Neuroglobin attenuates beta-amyloid neurotoxicity in vitro and transgenic Alzheimer phenotype in vivo. Proc Natl Acad Sci USA 104:19114–19119
69. Liu N, Yu Z, Xun Y, Shu P, Yue Y, Yuan S, Jiang Y, Huang Z, Yang X, Feng X, Xiang S, Wang X (2018) Amyloid-beta25-35 upregulates endogenous neuroprotectant neuroglobin via NFkappaB activation in vitro. J Alzheimers Dis 64:1163–1174
70. Zara S, De Colli M, Rapino M, Pacella S, Nasuti C, Sozio P, Di Stefano A, Cataldi A (2013) Ibuprofen and lipoic acid conjugate neuroprotective activity is mediated by Ngb/Akt intracellular signaling pathway in Alzheimer's disease rat model. Gerontology 59:250–260
71. Nicolis S, Monzani E, Pezzella A, Ascenzi P, Sbardella D, Casella L (2013) Neuroglobin modification by reactive quinone species. Chem Res Toxicol 26:1821–1831
72. Watanabe S, Takahashi N, Uchida H, Wakasugi K (2012) Human neuroglobin functions as an oxidative stress-responsive sensor for neuroprotection. J Biol Chem 287:30128–30138
73. Watanabe S, Wakasugi K (2008) Neuroprotective function of human neuroglobin is correlated with its guanine nucleotide dissociation inhibitor activity. Biochem Biophys Res Commun 369:695–700
74. Cai B, Li W, Mao X, Winters A, Ryou MG, Liu R, Greenberg DA, Wang N, Jin K, Yang SH (2015) Neuroglobin overexpression inhibits AMPK signaling and promotes cell anabolism. Mol Neurobiol 53:1254–1265
75. Yan W (2016) Carbon monoxide, the silent killer, may have met its match. Science 354:1215

76. Zou YY, Kan EM, Cao Q, Lu J, Ling EA (2013) Combustion smoke-induced inflammation in the cerebellum and hippocampus of adult rats. Neuropathol Appl Neurobiol 39:531–552
77. Warburton EC, Brown MW (2015) Neural circuitry for rat recognition memory. Behav Brain Res 285:131–139
78. Van Leuven W, Van Dam D, Moens L, De Deyn PP, Dewilde S (2013) A behavioural study of neuroglobin-overexpressing mice under normoxic and hypoxic conditions. Biochim Biophys Acta 1834:1764–1771
79. Lipovsek M, Grubb MS (2019) Boosting adult neurogenesis to enhance sensory performance. EMBO J 38:e101589
80. Goncalves JT, Schafer ST, Gage FH (2016) Adult neurogenesis in the hippocampus: from stem cells to behavior. Cell 167:897–914
81. Yu Z, Cheng C, Liu Y, Liu N, Lo EH, Wang X (2018) Neuroglobin promotes neurogenesis through Wnt signaling pathway. Cell Death Dis 9:945

Publisher's Note Springer Nature remains neutral with regard to jurisdictional claims in published maps and institutional affiliations.

Affiliations

Murat F. Gorgun[1] · Ming Zhuo[1] · Kelly T. Dineley[2,3,4] · Ella W. Englander[1,5]

Murat F. Gorgun
fmgorgun@utmb.edu

Ming Zhuo
mizhuo@utmb.edu

Kelly T. Dineley
ktdinele@utmb.edu

[1] Department of Surgery, Medical Branch, University of Texas, 301 University Boulevard, Galveston, TX 77555, USA

[2] Department of Neurology, University of Texas Medical Branch, Galveston, TX, USA

[3] Mitchell Center for Neurodegenerative Diseases, University of Texas Medical Branch, Galveston, TX, USA

[4] Center for Addiction Research, University of Texas Medical Branch, Galveston, TX, USA

[5] Shriners Hospitals for Children, Galveston, TX, USA